BSC

Design Calculation or Analysis Cover Sheet

Complete only applicable items.

3. System	4. Document Identifier
Monitored Geologic Repository	000-00C-MGR0-04100-000-00A

5. Title
TEV Collision with an Emplaced 5-DHLW/DOE SNF Short Co-Disposal Waste Package

6. Group
Thermal/Structural Analysis

7. Document Status Designation

☐ Preliminary ☒ Committed ☐ Confirmed ☐ Cancelled/Superseded

8. Notes/Comments

N/A

Attachments	Total Number of Pages
Attachment I – Figures obtained from LS-DYNA	2
Attachment II - Directory Listing of (Data CD) Electronic Files	3
Attachment III - Data CD Attachment, Electronic Files	N/A

RECORD OF REVISIONS

9. No.	10. Reason For Revision	11. Total # of Pgs.	12. Last Pg. #	13. Originator (Print/Sign/Date)	14. Checker (Print/Sign/Date)	15. EGS (Print/Sign/Date)	16. Approved/Accepted (Print/Sign/Date)
00A	Initial Issue.	33	33	Bryan Dunlap 8/30/07	Ken Jaquay 8/30/07	Jason Viggato 8/30/07	Michael Anderson 8/30/07
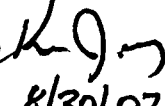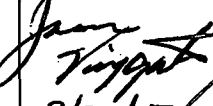
August 2007

DISCLAIMER

The calculations contained in this document were developed by Bechtel SAIC Company, LLC (BSC) and are intended solely for the use of BSC in its work for the Yucca Mountain Project.

TABLE OF CONTENTS

Page

TABLES

FIGURES

August 2007

ACRONYMS

ACC	Accession Number
ASM	American Society for Metals
ASME	American Society of Mechanical Engineers
ASTM	American Society for Testing and Materials
BSC	Bechtel SAIC Company, LLC.
CS	Carbon Steel
DHLW	Defense High Level Waste
DOE	United States Department of Energy
ED	Emplacement Drift
EP	Emplacement Pallet
FER.	Finite Element Representation
HP	Hewlett-Packard
LA	License Application
LSTC	Livermore Software Technology Corporation
MCO	Multicanister Overpack
OCB	Outer Corrosion Barrier
RT	Room Temperature
SI	Stress Intensity
SS	Stainless Steel
SNF	Spent Nuclear Fuel
TEV	Transport and Emplacement Vehicle
TIC	Technical Information Center reference number
WP	Waste Package

1. PURPOSE

The objective of this calculation is to determine the structural response of the 5-DHLW/DOE (Defense High Level Waste/Department of Energy) SNF (Spent Nuclear Fuel) Short Co-disposal Waste Package (WP) when subjected (while in the horizontal orientation emplaced in the drift) to a collision by a loaded (with WP) Transport and Emplacement Vehicle (TEV) due to an over-run. The scope of this calculation is limited to reporting the calculation results in terms of maximum total stress intensities (SIs) in the outer corrosion barrier (OCB).

The information regarding the dimensions of the WP and the short emplacement pallet (EP) used in this calculation are based on the drawings listed as References 2.2.6 to 2.2.8, and 2.2.12 to 2.2.23 respectively. Information regarding the general design and the envelope dimensions of the TEV are based on the figures and attachments in Reference 2.2.9. Room temperature (RT, $20\,°C\,(68\,°F)$) plastic material properties are used. Sensitivity studies in Reference 2.2.11, Section 6 indicate that temperature has negligible effect on the results of this type of calculation.

This calculation is intended for use in support of the preliminary design activities for the license application (LA) design of the WPs and performed by the Thermal/Structural Analysis Group.

2. REFERENCES

2.1. PROCEDURES/DIRECTIVES

2.1.1   DOE (U.S. Department of Energy) 2007. *Quality Management Directive.* QA-DIR-10, Rev. 001. Las Vegas, Nevada: Bechtel SAIC Company. ACC: DOC.20070330.0001.

2.1.2   EG-PRO-3DP-G04B-00037, Rev.9. *Calculations and Analyses.* Las Vegas, Nevada: Bechtel SAIC Company. ACC: ENG.20070717.0004.

2.1.3   IT-PRO-0011, Rev. 6. *Software Management.* Las Vegas, Nevada: Bechtel SAIC Company. ACC: DOC.20070802.0001.

2.1.4   ORD (Office of Repository Development) 2007. *Repository Project Management Automation Plan.* 000-PLN-MGR0-00200-000, Rev. 00E. Las Vegas, Nevada: U.S. Department of Energy, Office of Repository Development. ACC: ENG.20070326.0019.

2.2. DESIGN INPUTS

2.2.1   LS-DYNA V.3858 D MPP 2003. HP-UX 11.22. STN: 10300-970.3858 D MPP-00.

2.2.2   ASM (American Society for Metals) 1980. *Properties and Selection: Stainless Steels, Tool Materials and Special-Purpose Metals.* Volume 3 of *Metals Handbook.* 9th Edition. Benjamin, D., ed. Metals Park, Ohio: American Society for Metals. TIC: 209801. ISBN: 0-87170-009-3.

2.2.3 ASM International 1990. *Properties and Selection: Irons, Steels, and High-Performance Alloys*. Volume 1 of *Metals Handbook*. 10th Edition. Materials Park, Ohio: ASM International. TIC: 245666. ISBN: 0-87170-377-7.

2.2.4 ASME (American Society of Mechanical Engineers) 2001. *2001 ASME Boiler and Pressure Vessel Code (includes 2002 addenda)*. New York, New York: American Society of Mechanical Engineers. TIC: 251425.

2.2.5 ASTM (American Society for Testing and Materials) G 1-90 (Reapproved 1999). 1999. *Standard Practice for Preparing, Cleaning, and Evaluating Corrosion Test Specimens*. West Conshohocken, Pennsylvania: American Society for Testing and Materials. TIC: 238771.

2.2.6 BSC (Bechtel SAIC Company) 2007. *5-DHLW/DOE SNF - Short Co-Disposal Waste Package Configuration*. 000-MW0-DS00-00101-000-00D. Las Vegas, Nevada: Bechtel SAIC Company. ACC: ENG.20070719.0002.

2.2.7 BSC (Bechtel SAIC Company) 2007. *5-DHLW/DOE SNF - Short Co-Disposal Waste Package Configuration*. 000-MW0-DS00-00102-000-00C. Las Vegas, Nevada: Bechtel SAIC Company. ACC: ENG.20070719.0003.

2.2.8 BSC (Bechtel SAIC Company) 2007. *5-DHLW/DOE SNF - Short Co-Disposal Waste Package Configuration*. 000-MW0-DS00-00103-000-00C. Las Vegas, Nevada: Bechtel SAIC Company. ACC: ENG.20070719.0004.

2.2.9 BSC (Bechtel SAIC Company) 2007. *Transport and Emplacement Vehicle Envelope Calculation*. 800-MQC-HE00-00100-000-00B. Las Vegas, Nevada: Bechtel SAIC Company, ACC: ENG.20070830.0043.

2.2.10 BSC 2006. *Basis of Design for the TAD Canister-Based Repository Design Concept*. 000-3DR-MGR0-00300-000-000. Las Vegas, Nevada: Bechtel SAIC Company. ACC: ENG.20061023.0002.

2.2.11 BSC (Bechtel SAIC Company) 2004. *Design and Engineering, Stress Intensity Classification: Waste Package Outer Corrosion Barrier Stresses due to Horizontal Drop Event*. 000-00C-MGR0-01600-000-00A. Las Vegas, Nevada: Bechtel SAIC Company. ACC: ENG.20041122.0001.

2.2.12 BSC (Bechtel SAIC Company) 2004. *Design and Engineering, Emplacement Pallet Assembly Plate 1 [Sheet 4 of 15]*. 000-M00-SSE0-00304-000-00A. Las Vegas, Nevada: Bechtel SAIC Company. ACC: ENG.20040224.0008.

2.2.13 BSC (Bechtel SAIC Company) 2004. *Design and Engineering, Emplacement Pallet Assembly Plate 2 [Sheet 5 of 15]*. 000-M00-SSE0-00305-000-00A. Las Vegas, Nevada: Bechtel SAIC Company. ACC: ENG.20040224.0009.

2.2.14 BSC (Bechtel SAIC Company) 2004. *Design and Engineering Emplacement Pallet*

Assembly Plate 3 [Sheet 6 of 15]. 000-M00-SSE0-00306-000-00A. Las Vegas, Nevada: Bechtel SAIC Company. ACC: ENG.20040224.0010.

2.2.15 BSC (Bechtel SAIC Company) 2004. *Design and Engineering Emplacement Pallet Assembly Plate 4 [Sheet 7 of 15]*. 000-M00-SSE0-00307-000-00A. Las Vegas, Nevada: Bechtel SAIC Company. ACC: ENG.20040224.0011.

2.2.16 BSC (Bechtel SAIC Company) 2004. *Design and Engineering Emplacement Pallet Assembly Plate 5 [Sheet 8 of 15]*. 000-M00-SSE0-00308-000-00A. Las Vegas, Nevada: Bechtel SAIC Company. ACC: ENG.20040224.0012.

2.2.17 BSC (Bechtel SAIC Company) 2004. *Design and Engineering, Emplacement Pallet Assembly Plate 6 [Sheet 9 of 15]*. 000-M00-SSE0-00309-000-00A. Las Vegas, Nevada: Bechtel SAIC Company. ACC: ENG.20040224.0013.

2.2.18 BSC (Bechtel SAIC Company) 2004. *Design and Engineering, Emplacement Pallet Assembly Plate 7 [Sheet 10 of 15]*. 000-M00-SSE0-00310-000-00A. Las Vegas, Nevada: Bechtel SAIC Company. ACC: ENG.20040224.0014.

2.2.19 BSC (Bechtel SAIC Company) 2004. *Design and Engineering, Emplacement Pallet Assembly Plate 8 [Sheet 11 of 15]*. 000-M00-SSE0-00311-000-00A. Las Vegas, Nevada: Bechtel SAIC Company. ACC: ENG.20040224.0015.

2.2.20 BSC (Bechtel SAIC Company) 2004. *Design and Engineering, Emplacement Pallet Assembly Plate 9 [Sheet 12 of 15]*. 000-M00-SSE0-00312-000-00A. Las Vegas, Nevada: Bechtel SAIC Company. ACC: ENG.20040224.0016.

2.2.21 BSC (Bechtel SAIC Company) 2004. *Design and Engineering, Emplacement Pallet Assembly Tube 1 [Sheet 13 of 15]*. 000-M00-SSE0-00313-000-00A. Las Vegas, Nevada: Bechtel SAIC Company. ACC: ENG.20040224.0017.

2.2.22 BSC (Bechtel SAIC Company) 2004. *Design and Engineering, Emplacement Pallet Assembly Tube 2 [Sheet 14 of 15]*. 000-M00-SSE0-00314-000-00A. Las Vegas, Nevada: Bechtel SAIC Company. ACC: ENG.20040224.0018.

2.2.23 BSC (Bechtel SAIC Company) 2004. *Design and Engineering, Emplacement Pallet Assembly Tube 3 [Sheet 15 of 15]*. 000-M00-SSE0-00315-000-00A. Las Vegas, Nevada: Bechtel SAIC Company. ACC: ENG.20040224.0019.

2.2.24 Cummins, A.B. and Given, I.A. 1973. *SME Mining Engineering Handbook.* Two volumes. New York, New York: Society of Mining Engineers, American Institute of Mining, Metallurgical, and Petroleum Engineers. TIC: 210125.

2.2.25 DOE (U.S. Department of Energy) 2007. "High-Level Radioactive Waste and U.S. Department of Energy and Naval Spent Nuclear Fuel to the Civilian Radioactive Waste Management System." Volume 1 of *Integrated Interface Control Document.* DOE/RW-

0511, Rev. 3. Washington, D.C.: U.S. Department of Energy, Office of Civilian Radioactive Waste Management. ACC: DOC.20070125.0002.

2.2.26 DOE (U.S. Department of Energy) 2003. *Validation Test Report for LS-DYNA Version 970.3858 D MPP*. 10300-VTR-970.3858 D MPP-00. Las Vegas, Nevada: U.S. Department of Energy, Office of Repository Development. ACC: MOL.20031218.0337.

2.2.27 Haynes International. 1997. Hastelloy C-22 Alloy. Kokomo, Indiana: Haynes International. TIC: 238121.

2.2.28 Mecham, D.C., ed. 2004. *Waste Package Component Design Methodology Report*. 000-30R-WIS0-00100-000-002. Las Vegas, Nevada: Bechtel SAIC Company. ACC: ENG.20040713.0003.

2.2.29 Roark, R.J. and Young, W.C. 1975. *Formulas for Stress and Strain*. 5th Edition. New York, New York: McGraw-Hill. TIC: 240746. ISBN: 0-07-053031-9.

2.2.30 Not used.

2.2.31 BSC (Bechtel SAIC Company) 2007. *2-MCO/2-DHLW Waste Package Configuration*. 000-MW0-DS00-00301-000-00C. Las Vegas, Nevada: Bechtel SAIC Company. ACC: ENG.20070719.0008.

2.2.32 BSC (Bechtel SAIC Company) 2007. *2-MCO/2-DHLW Waste Package Configuration*. 000-MW0-DS00-00302-000-00C. Las Vegas, Nevada: Bechtel SAIC Company. ACC: ENG.20070719.0009.

2.2.33 BSC (Bechtel SAIC Company) 2007. *2-MCO/2-DHLW Waste Package Configuration*. 000-MW0-DS00-00303-000-00C. Las Vegas, Nevada: Bechtel SAIC Company. ACC: ENG.20070719.0010.

2.2.34 BSC (Bechtel SAIC Company) 2007. *Provisional Event Sequence Definitions for Waste Packages*. 000-30R-WIS0-00900-000-000. Las Vegas, Nevada: Bechtel SAIC Company. ACC: ENG.20070307.0014.

2.2.35 Boyer, H.E., ed. 2000. *Atlas of Stress-Strain Curves*. Metals Park, Ohio: ASM International. TIC: 248901. ISBN: 0-87170-240-1.

2.2.36 Nicholas, T. 1980. *Dynamic Tensile Testing of Structural Materials Using A Split Hopkinson Bar Apparatus*. AFWAL-TR-80-4053. Wright-Patterson Air Force Base, Ohio: Air Force Wright Aeronautical Laboratories. TIC: 249469.

2.2.37 LL020603612251.015. Slow Strain Rate Test Generated Stress Corrosion Cracking Data. Submittal date: 08/27/2002.

2.2.38 BSC (Bechtel SAIC Company) 2005. *IED Waste Package Processes, Ground Motion Time*

Histories, and Testing and Materials [Sheet 1 of 1]. 800-IED-WIS0-00501-000-00A. Las Vegas, Nevada: Bechtel SAIC Company, ACC: ENG.20050406.0004.

2.2.39   Avallone, E.A. and Baumeister, T., III, eds. 1987. *Marks' Standard Handbook for Mechanical Engineers.* 9th Edition. New York, New York: McGraw-Hill. TIC: 206891. ISBN: 0-07-004127-X.

2.2.40   Dieter, G.E. 1976. *Mechanical Metallurgy.* 2nd Edition. Materials Science and Engineering Series. New York, New York: McGraw-Hill Book Company. TIC: 247879. ISBN: 0-07-016891-1.

2.2.41   BSC (Bechtel SAIC Company) 2007. *IED Emplacement Drift Configuration and Environment.* 800-IED-MGR0-00501-000-00B. Las Vegas, Nevada: Bechtel SAIC Company, ACC: ENG.20070716.0006.

2.3.   DESIGN CONSTRAINTS

None.

2.4.   DESIGN OUTPUTS

Results from this calculation will be used by the Subsurface Engineering Organization in other calculations and analyses.

Results from this calculation are expected to be used in the *HLW/DOE SNF Codisposal Waste Package Design Report*, 000-00C-DS00-00600-000-00C.

3. ASSUMPTIONS

The following assumptions are made regarding the analysis of a TEV collision with an emplaced WP, specifically the 5-DHLW/DOE SNF Short Co-disposal WP, which is then pushed into another emplaced WP, specifically a restrained 2-MCO/2-DHLW WP.

3.1.   ASSUMPTIONS REQUIRING VERIFICATION

3.1.1   The dimensions, masses, materials and load paths of the WPs and EP used in the development of this calculation, corresponding to the drawings and of References 2.2.6 to 2.2.8 (5-DHLW/DOE SNF Short Co-disposal WP), 2.2.31 to 2.2.33 (2-MCO/2-DHLW WP), 2.2.12 to 2.2.23 (EP) and 2.2.9 (TEV) are assumed to be reasonably the same in the regions of high stress and load transfer as the final definitive design. The rationale for this assumption is that the design of References 2.2.6 to 2.2.8, 2.2.31 to 2.2.33, 2.2.12 to 2.2.23 and 2.2.9, in the region of high stress and load transfer, is representative of the design created for the LA. This assumption is used in Section 6.3 and will require verification at completion of the final definitive design.

3.1.2   The design basis velocity for the TEV is approximated to be 2 *mph* (0.894 *m/s*) to provide for a conservative bounding force due to impact (maximum velocity of the TEV is 1.705 *mph* (0.762 *m/s*) per Reference 2.2.9, Section 6.7.3). This assumption is used in Sections 6.2 and 6.3 and will require verification at completion of the final definitive design.

3.1.3   The driving force calculated in Section 6.2 is assumed to be the upper bound of the driving force the TEV motors will produce during a collision with an emplaced WP event sequence. First the tractive effort required for normal operation of the TEV is calculated and then a design factor is applied to derive the bounding driving force that could be produced by the TEV motors. A design factor of 50% over the required tractive effort will be used to create a bounding condition for the driving force supplied by the TEV motors. The assumption for the bounding driving force produced by the TEV is used in Section 6.3 and will have to be verified as a bounding driving force at the completion of the final definitive design for the TEV.

3.2.   ASSUMPTIONS NOT REQUIRING VERIFICATION

3.2.1   Strain-rate-dependent material properties are not available for ASME SB-575 [UNS N06022], ASME SA-240 [UNS S31600, with modified N & C], ASME SA-516 [UNS K02700], ASME SA-240 [UNS S31603], and ASME SA-240 [UNS S30403], hereinafter termed Alloy 22, 316 stainless steel (SS), 516 carbon steel (CS), 316L SS, and 304L SS. The material properties obtained under static loading conditions are assumed for these materials. Figure 1 is a time plot in seconds (s) of the wall-averaged effective plastic strain at the OCB location in the impacted WP with the highest wall-averaged stress intensity. From Figure 1 the maximum wall averaged effective plastic strain rate (maximum slope of the plastic strain curve) is seen to be 0.3 s^{-1}. For this value of strain rate, Reference 2.2.36 Figures 27 and 30, pages 42 and 45, respectively, indicates a negligible strengthening of the 300 Series stainless steel and high alloy steels. Therefore, the impact of using material properties obtained under static loading conditions in this calculation is anticipated to be small and therefore this assumption does not require verification. This assumption is used in Section 6.1.
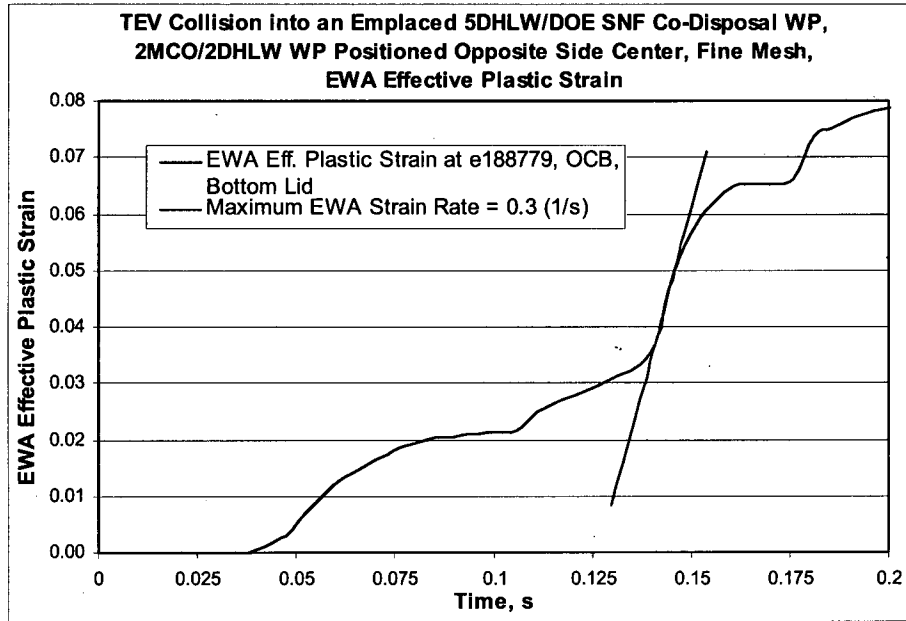
Figure 1.   EWA Effective Plastic Strain in Lower OCB Lid During a TEV Collision With an
Emplaced WP

3.2.2   The RT Poisson's ratio of Alloy 22 is not published in traditional sources. Therefore, the Poisson's ratio of ASME SB-443 [UNS N06625], hereinafter termed Alloy 625, is assumed for Alloy 22. The chemical composition of Alloy 22 and Alloy 625 are similar since they are both 600 Series nickel-base alloys (Reference 2.2.4, Section II, Part B, SB-575, Table 1 and Reference 2.2.2, p. 143, respectively). Therefore, the difference in their Poisson's ratio is expected to be small. The rationale for this expectation is that Reference 2.2.2, pages 141, 143 and 145 indicate small difference in RT Poisson ratio values for the 600 Series nickel-base alloy family:

Alloy 600 [UNS N06600] = 0.290
Alloy 625 [UNS N06625] = 0.278
Alloy 690 [UNS N06690] = 0.289

The impact on stress results of small differences in Poisson's ratio is anticipated to be negligible. The rationale for this anticipation is that Reference 2.2.29 Table 30 stress formulas for cylindrical shells indicate insensitivity to Poisson's ratio. For the loading case of uniform radial shear loads (Case 8), the key breaching stress, the maximum hoop circumferential membrane stress, is proportional to Poisson's Ratio, υ, through the term $(1-\upsilon^2)^{1/4}$. Using the lowest and highest values of the three 600 Series nickel-base alloy υ values, 0.278 and 0.290, the difference in maximum hoop circumferential membrane stress values, all things being equal except υ, is a negligible 0.2%. Therefore, this study of parametric variations provides verification of this assumption per Reference 2.1.2, page 4 (*"Verification may include ... studies of parametric variations"*) and further verification of this assumption is not required. This assumption is used in Section 6.1 and is consistent with Section 5.2.8.2 of Reference 2.2.28.

3.2.3 The RT Poisson's ratio of 316L SS is not published in traditional sources. Therefore, the RT Poisson's ratio of 316 SS is assumed for 316L SS. The chemical compositions of 316L SS and 316 SS are similar (Reference 2.2.4, Section II, Part A, SA-240, Table 1) because they are both 300 Series (austenitic) stainless steels. Therefore, the difference in their Poisson's ratio is expected to be small. The rationale for this expectation is that Reference 2.2.2 page 755 Figure 15 indicates small differences in RT Poisson ratio values for the 300 Series SS family:

Type 304 SS [UNS S30400] = 0.290
Type 316 SS [UNS S31600] = 0.298
Type 310 SS [UNS S31000] = 0.308

The impact on stress results of small differences in Poisson's ratio is anticipated to be negligible. The rationale for this anticipation is that the Reference 2.2.29, Table 30 stress formulas for cylindrical shells indicate insensitivity to Poisson's ratio. For the loading case of uniform radial shear loads (Case 8), the key breaching stress, the maximum hoop circumferential membrane stress, is proportional to Poisson's ratio, υ, through the term $(1-\upsilon^2)^{1/4}$. Using the lowest and highest values of the three 300 Series SS Poisson's ratio υ values, 0.290 and 0.308, the difference in maximum hoop circumferential membrane stress values, all things being equal except υ, is a negligible 0.3%. Therefore, this study of parametric variations provides verification of this assumption per Reference 2.1.2, page 4 (*"Verification may include . . . studies of parametric variations"*) and further verification of this assumption is not required. This assumption is used in Section 6.1 and is consistent with Section 5.2.8.4, of Reference 2.2.28.

3.2.4 The RT uniform strain of 316L SS (strain corresponding to tensile strength) is not listed in traditional sources. Therefore, it is assumed that the RT uniform strain is 60% of the RT minimum specified elongation (strain corresponding to rupture point in tensile test). The rationale for this assumption is graphical measurements of a stress-strain curve for "as-received" 316L SS material at a moderate strain rate, 8 s^{-1} (Reference 2.2.35, p. 305). Therefore this assumption does not require verification. This assumption is used in Section 6.1 and corresponds to Section 5.2.6.2 in Reference 2.2.28.

3.2.5 The RT uniform strain of Alloy 22 is not listed in traditional sources. Therefore, it is assumed that the RT uniform strain is 90% of the RT minimum specified elongation for Alloy 22. The rationale for this assumption is based on measurements of RT stress-strain curves for Alloy 22 (DTN: LL0206036122551.015, Ref. 2.2.37). The use of Reference 2.2.37 was approved as the appropriate data for the intended use in an Information Exchange Document (Reference 2.2.38). Therefore this assumption does not require verification. This assumption is used in Section 6.1 and corresponds to Section 5.2.6.3 in Reference 2.2.28.

3.2.6 The RT uniform strain of 316 SS is not listed in traditional sources. Therefore, it is assumed that the RT uniform strain is 90% of the RT minimum specified elongation. The rationale for this assumption is based on measurements of the RT stress-strain curve for 316 SS from a qualified source (Reference 2.2.35, p. 304). Therefore this assumption does not require

verification. This assumption is used in Section 6.1 and corresponds to Section 5.2.6.3 in Reference 2.2.28.

3.2.7   The RT uniform strain of 304L SS is not listed in traditional sources. Therefore, it is assumed that the uniform strain is 75% of the minimum specified elongation. The rationale for this assumption is based on the measurements of the RT stress-strain curve for 304 SS (Reference 2.2.35, p. 294), which has a similar chemical composition to 304L SS (Reference 2.2.4, Section II, Part A, SA-240, Table 1). Use of this assumption is limited to the DHLW canister conceptualization in the 5-DHLW/DOE SNF Short Co-disposal WP whose behavior will have an insignificant effect on the OCB structural response. Therefore this assumption does not require verification. This assumption is used in Section 6.1.

3.2.8   The friction coefficients for contacts among the Alloy 22 components, or the contacts involving Alloy 22 and other metallic materials, are not available in traditional sources. It is, therefore, assumed that the dynamic (sliding) friction coefficient for both of these contacts is 0.4. The rationale for this assumption is that this friction coefficient represents the lower (conservative – less energy loss due to WP internal component contact) bound for most dry nickel-on-steel and nickel-on-nickel contacts (Reference 2.2.39, Table 3.2.1, p. 3-26); nickel being the dominant component in Alloy 22 (Reference 2.2.4, Section II, Part B, SB-575, Table 1). Therefore this assumption does not require verification. This assumption is used in Section 6.3 and corresponds to Section 5.2.14.1 in Reference 2.2.28.

3.2.9   The variation of functional friction coefficient between the static and dynamic value as a function of relative velocity of the surfaces in contact is not available in traditional sources for the materials used in this calculation. Therefore, the effect of relative velocity of the surfaces in contact is neglected in these calculations by assuming that the functional friction coefficients and static friction coefficients are both equal to the dynamic friction coefficient. The impact of this assumption on results presented in this document is anticipated to be negligible. The rationale for this assumption is that it provides a conservative bounding set of results by minimizing the friction coefficient within the given finite element analysis framework. Therefore this assumption does not require verification. This assumption is used in Section 6.3 and corresponds to Section 5.2.14.2 in Reference 2.2.28.

3.2.10 The RT Poisson's ratio for 304L SS is not published in traditional sources. Therefore, it is assumed to be the same as the Poisson's ratio for 304 SS (Reference 2.2.2, Figure 15, p. 755). The rationale for this assumption is that the chemical compositions of 304L stainless steel and 304 stainless steel are similar (Reference 2.2.4, Section II, Part A, SA-240, Table 1) because they are both 300 Series (austenitic) stainless steels. Therefore the differences in their Poisson's ratio values are expected to be small. The 300 Series stainless steels have a relatively small range of RT Poisson ratio values that leads to negligible stress effect as shown by studies of parametric variations (see Assumption 3.2.3). Further verification of this assumption is not required. This assumption is used in Section 6.1 and corresponds to Section 5.2.8.5 in Reference 2.2.28.

3.2.11 The RT uniform strain of A 516 CS is not published in traditional sources. Therefore, it is conservatively assumed that the uniform strain is 50 percent of the elongation. The rationale

for this assumption is geometric measurements of the stress-strain curve for A 36 CS (Reference 2.2.35, p. 186), which has a similar chemical composition as A 516 CS (Reference 2.2.4, Section II, Part A, SA-516/SA-516M, Table 1 and SA-36/SA-36M, Table 2). Use of this assumption is limited to the waste form basket structure whose behavior will have an insignificant effect on the OCB structural response. Therefore this assumption does not require verification. This assumption is used in Section 6.1 and corresponds to Section 5.2.6.1 in Reference 2.2.28.

3.2.12   The use of a 2-MCO/2-DHLW WP on the opposite end of the 5-DHLW/DOE SNF Short Co-disposal WP impacted by the over-driven TEV will produce a conservative structural response. The orientation of the neighboring WP, as well as, the size of the neighboring WP will have an effect on the structural response of the 5-DHLW/DOE SNF Short Co-disposal WP. The rationale for this assumption is that the 2-MCO/2-DHLW WP has the smallest diameter (Reference 2.2.32) of the types of WPs expected to be emplaced in the repository and because of the smaller diameter it is expected to create a smaller area of contact and higher concentration of the collision force to produce a higher structural response in the 5-DHLW/DOE SNF Short Co-disposal WP. Therefore this assumption does not require verification. This assumption is used in Sections 6.3 and 6.4.

3.2.13   Orientation of the WP on the opposite end of the 5-DHLW/DOE SNF Short Co-disposal WP impacted by the over-driven TEV by 30° off of the emplacement drift axis will produce a conservative structural response. As calculated in Section 6.4 a 2-MCO/2-DHLW WP pushed off of the emplacement drift axis by a WP being pushed into it by an over-driven TEV could get to an extreme angle of 30° off the emplacement drift axis. Using the 30° angle of attack for the 2-MCO/2-DHLW WP on the opposite end of the 5-DHLW/DOE SNF Short Co-disposal WP impacted by the over-driven TEV is assumed to produce a bounding structural response in the 5-DHLW/DOE SNF Short Co-disposal WP because of its smaller contact area and higher concentration of the collision force when compared to shallower angles. Therefore this assumption does not require verification. This assumption is used in Section 6.3.

3.2.14   Conceptualization of the TEV as a simple plate with material properties of A 516 CS will produce a conservative structural response by the impacted WP. Since only the structural response of the OCB is of interest the TEV can be simplified to a plate assigned the mass of a fully loaded TEV. The TEV front door plate conceptualization included plastic material behavior and the material properties assigned were that of A 516 CS which has a typical steel modulus of elasticity (Section 6.1) and a relatively high yield strength of 262 *MPa* (38.0 *ksi*) (Section 6.1). This selection of element type and material properties was based on achieving a more realistic behavior than would be achieved by simply using a rigid or elastic element type while also insuring a bounding strength of material behavior until the TEV final definitive design is submitted. Therefore this assumption does not require verification. This assumption is used in Section 6.3.

4. METHODOLOGY

4.1.   QUALITY ASSURANCE

This calculation is associated with the WP design and is performed by the Thermal/Structural Analysis Group in accordance with EG-PRO-3DP-G04B-00037, *Calculations and Analyses* (Reference 2.1.2). WPs are classified as safety category (important to safety and important to waste isolation) items (Reference 2.2.10, Section 11.1.2). The TEV is classified as a safety category (important to safety) item (Reference 2.2.10, Section 14.1.2). Therefore, this document is subject to requirements of the BSC *Quality Management Directive* (Reference 2.1.1, Section 2.1.C.1.1.a.i and 17.E) and the approved version is designated as QA: QA.

4.2.   USE OF SOFTWARE

The computer code used for dynamic structural analysis in this calculation is the commercially available LS-DYNA V.970.3858 D MPP finite element analysis package (Software Tracking Number (STN): 10300-970.3858 D MPP-00, Ref. 2.2.1). The LS-DYNA software package is obtained from Software Configuration Management in accordance with IT-PRO-0011, *Software Management* (Reference 2.1.3). This version of the LS-DYNA code has an available validation test report (Reference 2.2.26) and the evaluation performed for this calculation is fully within the range of the validation performed for the code. LS-DYNA is appropriate for the WP structural analyses performed in this calculation. The simulations were all performed on a Hewlett-Packard (HP) Itanium2 platform cluster which uses the HP-UX 11.22 operating system. The HP Itanium2 platform computer cluster is identified with one tag number: 501711. All workstations are located in Las Vegas, Nevada. LS-DYNA is listed in the *Repository Project Management Automation Plan* (Reference 2.1.4, Table 6-1). The results of this calculation are provided in terms of stress intensities.

The commercially available TrueGrid V2.2 (Software Tracking Number 610418-2.2.0-00) meshing code, hereinafter referred to as "TrueGrid", is used in this calculation solely to mesh geometric representations of the WP in the simulations. TrueGrid is a pre-processing tool for graphical and geometrical representation and therefore is Level 2 software as defined in *Software Management* (Reference 2.1.3, Section 4 and Attachment 12). The meshing is executed on the Hewlett-Packard 9000 series UNIX workstation (Operating System HP-UX 11.0), identified with Yucca Mountain Project tag number 150690, located in Las Vegas, Nevada. The suitability and adequacy of the mesh generated using TrueGrid is based on visual examination, engineering judgment, and the results of the mesh verification exercise performed in section 7.1. TrueGrid is listed in the *Repository Project Management Automation Plan* (Reference 2.1.4, Table 6-1).

LS-PREPOST V1.0 (Livermore Software Technology Corporation) is the postprocessor used only for visual display and graphical representation of LS-DYNA FERs and results and therefore is Level 2 software as defined in Reference 2.1.3, Attachment 12. The suitability and adequacy of the displayed results is based on visual examination and engineering judgment. The post processing is performed on HP Itanium2 (IA64) series UNIX workstations (Operating System HP-UX 11.22), collectively identified with the Yucca Mountain Project tag number 501711, and located in Las Vegas, Nevada. LS-PREPOST is listed in the *Repository Project Management Automation Plan* (Reference 2.1.4, Table 6-1).

The commercially available Microsoft Office Excel 2003 (11.8105.8107 SP2) spreadsheet code, which is a component of Microsoft Office 2003 Professional, is used to perform simple data conversion (maximum shear stress to stress intensity) and plotting. These results were verified by checks using hand calculations and plots were verified by visual inspection. Usage of Microsoft Office 2003 Professional in this calculation constitutes Level 2 software usage, as defined in IT-PRO-0011 (Reference 2.1.3, Section 4 and Attachment 12). Microsoft Office 2003 Professional is listed in the *Repository Project Management Automation Plan* (Reference 2.1.4, Table 6-1). Microsoft Office Excel 2003 was executed on a PC with X86 architecture running the Microsoft Windows XP Professional operating system, Version 5.1.2600, Service Pack 2, Build 2600.

The LS-DYNA, Truegrid, and Microsoft Excel electronic files are provided in Attachment III.

4.3.   APPROACH

An explicit finite element analysis of the structural response of an emplaced waste package that is impacted on its upper lid by a fully loaded TEV is performed. The TEV is over-driven and an impact with the emplaced WP is modeled to occur with the TEV doors closed, at full speed and with full power applied to the drive motors in this event sequence (Reference 2.2.34, Section 4.3.6). The TEV Collision with an Emplaced WP event sequence is not described in the current *Basis of Design for the TAD Canister-Based Repository Design Concept* (Reference 2.2.10), therefore, the event sequence description provided in *Provisional Event Sequence Definitions for Waste Packages* (Reference 2.2.34) is suitable for its intended use in this calculation. The driving force imparted by the TEV onto the WP is determined by first estimating the tractive effort required for normal operation of the TEV. Using the tractive effort required and a factor of safety multiplier, a total force for the driving motors may be approximated that is transferred over the area of impact for the WP. The tractive effort and total driving force required for the normal operation of the TEV are derived by a hand calculation, see Section 6.2.

The emplaced WP that is impacted by the TEV has its lower lid driven into a neighboring emplaced WP. The neighboring emplaced WP is assumed to get displaced by the movement into a position that is structurally challenging to the emplaced WP that is driven into it. The neighboring WP is used as a boundary condition to the TEV collision model and is statically positioned at a 30° angle, as determined in the hand calculation performed in Section 6.4, to the emplaced WP in between it and the TEV. Because the relative position of the neighboring WP to the impacted WP has considerable variability, two relative positions of the contacting edge of the neighboring WP with the bottom of the impacted WP were considered. The contacting edge position of the neighboring WP located in the center of the bottom lid of the impacted WP's OCB should be the most structurally challenging location. To confirm that the center location was the most structurally challenging location for the contacting edge of the neighboring WP another contact location on the impacted WP's bottom lid was simulated.

The mesh discretization level was verified as adequate for this analysis using the mesh optimization technique described in the *Waste Package Component Design Methodology Report* (Reference 2.2.28, Section 6.2.3).

Hand calculations were performed to interpolate material properties from available data, see

Section 6.1.2, and to derive the Tangent Moduli of the materials used in the LS-DYNA models, see Section 6.1.3.

The scope of this calculation will be limited to reporting the structural response of the OCB of the impacted WP in the form of stress intensities (SIs). If failure criterion screening using the calculated SIs in the OCB are not met (Reference 2.2.28, Section 6.2.4) then the OCB is considered breached and the WP is considered failed.

5. ATTACHMENTS

		Number of Pages
Attachment I.	Figures obtained from LS-DYNA	2
Attachment II.	Directory Listing of (Data CD) Electronic Files	3
Attachment III.	Data CD Attachment	Electronic file, 1 disk

6. BODY OF CALCULATION

6.1. MATERIAL PROPERTIES

The RT elastic material properties used in these calculations are listed in this section. All material properties listed below are obtained under static loading conditions (see Assumptions 3.2.1, 3.2.2, 3.2.3, and 3.2.10).

Stress units are Pascal (Pa), Mega Pascal ($MPa = 10^6 Pa$), Giga Pascal ($GPa = 10^9 Pa$), lb/in^2 (psi) and $ksi = 10^3 psi$.

6.1.1. Listing of Material Properties

Unless noted, the material properties listed in this section are at room temperature.

Alloy 22 [ASME SB-575 UNS N06022] (EP and OCB):

- Density = 8690 kg/m^3 (0.314 lb/in^3)
    (Reference 2.2.4, Section II, Part B, SB-575, Section 7.1)
- Poisson's ratio = 0.278
    (Assumption 3.2.2)
- Elongation = 0.45
    (Reference 2.2.4, Section II, Part B, SB-575, Table 4)
- Modulus of Elasticity = 206 GPa (29.9 x $10^6 psi$)
    (Reference 2.2.27, p.14, Table "Average Dynamic Modulus of Elasticity")
    This data is the best available and suitable for its use in this calculation.
- Yield Strength = 310 MPa (45.0 ksi)
    (Reference 2.2.4, Section II, Part D, Subpart 1, Table Y-1)
- Tensile Strength = 689 MPa (100 ksi)

(Reference 2.2.4, Section II, Part D, Subpart 1, Table U)

316 SS [ASME SA-240 UNS S31600] (EP Tube 1s, Interface ring, Inner vessel and Shear ring):

- Density = 7980 kg/m^3 (0.288 lb/in^3)
  (Reference 2.2.5, Table X1.1, p. 7)
- Poisson's ratio = 0.298
  (Reference 2.2.2, Figure 15, p. 755)
- Elongation = 0.40
  (Reference 2.2.4, Section II, Part A, SA-240, Table 2)
- Modulus of Elasticity = 195 GPa (28.3·10^6 psi)
  (Reference 2.2.4, Section II, Part D, Subpart 2, Table TM-1)
- Yield Strength = 207 MPa (30.0 ksi)
  (Reference 2.2.4, Section II, Part D, Subpart 1, Table Y-1)
- Tensile Strength = 517 MPa (75.0 ksi)
  (Reference 2.2.4, Section II, Part D, Subpart 1, Table U)

316L SS [ASME SA-240 UNS S31603]
  (DOE SNF canister, Reference 2.2.10, Section 11.2.2.8):

- Density = 7980 kg/m^3 (0.288 lb/in^3)
  (Reference 2.2.5, Table X1.1, p. 7)
- Poisson's ratio = 0.298
  (Assumption 3.2.3)
- Elongation = 0.40
  (Reference 2.2.4, Section II, Part A, SA-240, Table 2)
- Modulus of Elasticity = 195 GPa (28.3·10^6 psi)
  (Reference 2.2.4, Section II, Part D, Subpart 2, Table TM-1)
- Yield Strength = 172 MPa (25.0 ksi)
  (Reference 2.2.4, Section II, Part D, Subpart 1, Table Y-1)
- Tensile Strength = 483 MPa (70.0 ksi)
  (Reference 2.2.4, Section II, Part D, Subpart 1, Table U)

304L SS [ASME SA-240 UNS S30403]
  (HLW canisters, Reference 2.2.10, Section 11.2.2.7):

- Density = 7980 kg/m^3 (0.288 lb/in^3)
  (Reference 2.2.5, Table X1.1, p. 7)
- Poisson's ratio = 0.29
  (Assumption 3.2.10)
- Elongation = 0.40
  (Reference 2.2.4, Section II, Part A, SA-240, Table 2)
- Modulus of Elasticity = 195 GPa (28.3·10^6 psi)
  (Reference 2.2.4, Section II, Part D, Subpart 2, Table TM-1)
- Yield Strength = 172 MPa (25.0 ksi)

(Reference 2.2.4, Section II, Part D, Subpart 1, Table Y-1)
- Tensile Strength = 483 *MPa* (70.0 *ksi*)
    (Reference 2.2.4, Section II, Part D, Subpart 1, Table U)

A 516 CS [ASME SA-516 UNS K02700]
    (Divider Plate Assembly and TEV Conceptualization):

- Density = 7850 *kg/m³* (0.284 *lb/in³*)
    (Reference 2.2.4, Section II, Part A, SA-20/SA20M, Section 14.1)
- Poisson's ratio = 0.30
    (Reference 2.2.3, p. 374)
- Elongation = 0.21
    (Reference 2.2.4, Section II, Part A, SA-516/SA-516M, Table 2)
- Modulus of Elasticity = 203 *GPa* (29.5·10⁶ *psi*)
    (Reference 2.2.4, Section II, Part D, Subpart 2, Table TM-1)
- Yield Strength = 262 *MPa* (38.0 *ksi*)
    (Reference 2.2.4, Section II, Part D, Subpart 1, Table Y-1)
- Tensile Strength = 483 *MPa* (70.0 *ksi*)
    (Reference 2.2.4, Section II, Part D, Subpart 1, Table U)

6.1.2. Calculations for True Measure of Ductility

The material properties in Section 6.1.1 refer to engineering stress and strain definitions: $S = P / A_0$ and $e = (L - L_0) / L_0$ (see Reference 2.2.40, Chapter 9). Where P stands for the force applied during a static tensile test, L is the length of the deformed specimen, and L_0 and A_0 are the original length and cross-sectional area of the specimen, respectively. The engineering stress-strain curve does not give a true indication of the deformation characteristics of a material during plastic deformation since it is based entirely on the original dimensions of the specimen. Hence, the constitutive relation in LS-DYNA is defined in terms of true stress and strain: $\sigma = P / A$ and $\varepsilon = \ln(L / L_0)$ where A is the deformed area (Reference 2.2.40, Chapter 9).

The relationships between the true stress and strain definitions and the engineering stress and strain definitions, $\sigma = S(1 + e)$ and $\varepsilon = \ln(1 + e)$, can be readily derived based on constancy of volume ($A_0 L_0 = AL$) and strain homogeneity during plastic deformation (Reference 2.2.40, Chapter 9). These expressions are applicable only in the hardening region of the stress-strain curve that is limited by the onset of necking.

The following parameters are used in the subsequent calculations:
$S_y \cong \sigma_y$ = yield strength
S_u = engineering tensile strength
σ_u = true tensile strength
$e_y \cong \varepsilon_y$ = strain corresponding to yield strength
e_u = engineering strain corresponding to tensile strength (engineering uniform strain)
ε_u = true strain corresponding to tensile strength (true uniform strain)

In absence of data on the uniform strain in traditional sources, the uniform strain needs to be empirically derived based on the shape of stress-strain curves and elongation data (strain corresponding to rupture of the tensile specimen).

For Alloy 22 and 316 SS, a reduction in RT elongation by 10% is assumed for the RT uniform strain (see Assumptions 3.2.5 and 3.2.6).

For Alloy 22;
$e_u = 0.9 *$ Elongation $= 0.9 * 0.45 = 0.41$
$\varepsilon_u = \ln (1 + e_u) = \ln (1 + 0.41) = 0.34$
$\sigma_u = S_u (1 + e_u) = 689 (1 + 0.41) = 971$ *MPa* (141 *ksi*)
Therefore, the true tensile strength of Alloy 22 at RT is 971 *MPa* (141 *ksi*).

For 316 SS;
$e_u = 0.9 *$ Elongation $= 0.9 * 0.40 = 0.36$
$\varepsilon_u = \ln (1 + e_u) = \ln (1 + 0.36) = 0.31$
$\sigma_u = S_u (1 + e_u) = 517 (1 + 0.36) = 703$ *MPa* (102 *ksi*)
Therefore, the true tensile strength of 316 SS at RT is 703 *MPa* (102 *ksi*).

For 316L SS the RT uniform strain is assumed to be 60% of RT elongation (see Assumption 3.2.4).
$e_u = 0.6 *$ Elongation $= 0.6 * 0.40 = 0.24$
$\varepsilon_u = \ln (1 + e_u) = \ln (1 + 0.24) = 0.22$
$\sigma_u = S_u (1 + e_u) = 483 (1 + 0.24) = 599$ *MPa* (86.9 *ksi*)
Therefore, the true tensile strength of 316L SS at RT is 599 *MPa* (86.9 *ksi*).

For 304L SS the RT uniform strain is assumed to be 75% of the RT elongation value for 304 SS (see Assumption 3.2.7).
$e_u = 0.75 *$ Elongation $= 0.75 * 0.40 = 0.30$
$\varepsilon_u = \ln (1 + e_u) = \ln (1 + 0.30) = 0.26$
$\sigma_u = S_u (1 + e_u) = 483 (1 + 0.30) = 628$ *MPa* (91.1 *ksi*)
Therefore, the true tensile strength of 304L SS at RT is 628 *MPa* (91.1 *ksi*).

For A 516 CS the RT uniform strain is assumed to be 50% of the RT elongation value for A 36 CS (see Assumption 3.2.11).
$e_u = 0.5 *$ Elongation $= 0.5 * 0.21 = 0.11$
$\varepsilon_u = \ln (1 + e_u) = \ln (1 + 0.11) = 0.10$
$\sigma_u = S_u (1 + e_u) = 483 (1 + 0.11) = 536$ *MPa* (77.7 *ksi*)
Therefore, the true tensile strength of A 516 CS at RT is 536 *MPa* (77.7 *ksi*).

6.1.3. Calculations for Tangent Moduli

The results of this simulation are required to include elastic and plastic deformations for all materials. When the materials are driven into the plastic range, the slope of the stress-strain curve continuously changes. A ductile failure is preceded by a protracted regime of hardening and

substantial accumulation of inelastic strains. Thus, a simplification for the stress-strain curve is needed to incorporate plasticity into the FEA. A standard approximation commonly used in engineering is to use a straight line that connects the yield point and the tensile strength point of the material. The parameters used in the subsequent calculations in addition to those defined in Section 6.1.2 are modulus of elasticity (E) and tangent (hardening) modulus (E_1). The tangent modulus represents the slope of the stress-strain curve in the plastic region.

For Alloy 22 (used in OCB, WP Sleeves, and EP Base), the tangent modulus at RT is calculated using the true stress and strain values derived in Sections 6.1.1 and 6.1.2:
$$E_1 = (\sigma_u - \sigma_y) / (\varepsilon_u - \sigma_y / E) = (0.971 - 0.310) / (0.34 - 0.310 / 206) = 1.95 \text{ GPa (283 ksi)}$$

For 316 SS (used in Inner Vessel and EP Longitudinal Posts) at RT:
$$E_1 = (\sigma_u - \sigma_y) / (\varepsilon_u - \sigma_y / E) = (0.703 - 0.207) / (0.31 - 0.207 / 195) = 1.60 \text{ GPa (232 ksi)}$$

For 316L SS (used in DOE SNF Canister) at RT:
$$E_1 = (\sigma_u - \sigma_y) / (\varepsilon_u - \sigma_y / E) = (0.599 - 0.172) / (0.22 - 0.172 / 195) = 1.95 \text{ GPa (283 ksi)}$$

For 304L SS (used in DHLW Canister) at RT:
$$E_1 = (\sigma_u - \sigma_y) / (\varepsilon_u - \sigma_y / E) = (0.628 - 0.172) / (0.26 - 0.172 / 195) = 1.76 \text{ GPa (255 ksi)}$$

For A516 CS (used in Divider Plates and TEV Door Conceptualization) at RT:
$$E_1 = (\sigma_u - \sigma_y) / (\varepsilon_u - \sigma_y / E) = (0.536 - 0.262) / (0.10 - 0.262 / 203) = 2.78 \text{ GPa (403 ksi)}$$

6.2.   TEV DRIVING FORCE

The total driving force exerted on the impacted WP will be equal to that generated by the TEV in order to propel itself at a speed 2.0 *mph* (0.894 *m/s*) (Assumption 3.1.2). The TEV force generated and then transferred to the impacted WP is found by first calculating the tractive effort required by the fully loaded, 300 *ton* (272,000 *kg*), vehicle (Reference 2.2.9, Section 7.8). Equation 6.1 calculates the tractive effort (*lbs* of force) required to move the TEV in a straight line (Reference 2.2.24, pages 14-10 and 14-11), and includes the total weight, frictional resistance and grade resistance.

$$TE = WR_w + LR + TgG + TaA \qquad \text{Equation 6.1}$$

where:

L is the trailing load in *tons* (no trailer $\therefore L = 0$)
W is the TEV weight in *tons*
T is the total weight $(W + L) = W$ in *tons*
g is the percent grade
G is the grade resistance – Approximately 20 *lbf / ton / % grade* (Ref. 2.2.24, pg. 14-10)
R_w is the frictional resistance of the TEV – Approx. *20 lbf / ton* (Ref. 2.2.24, pg. 14-10)
R is the frictional resistance of a coupled train in *lbf / ton* (no trailer $\therefore R = 0$)
a is the rate of acceleration in *mph / sec²* – Approx. 0.2 *mph / sec²* (Ref. 2.2.24, pg. 14-10)

A is the accelerating force – Approx. 100 lb / ton / (1 mph / sec^2) (Ref. 2.2.24, pg. 14-10)
TE is the tractive effort of the TEV in lb_f

Using a design percent grade, g, of 2.5 percent (Reference 2.2.10, Section 9.9.2.2.4) and solving Equation 6.1 results in a tractive effort of 27,000 lb_f (120,000 N).

$$TE = 300 \cdot 20 + 0 \cdot R + 300 \cdot 2.5 \cdot 20 + 300 \cdot 0.2 \cdot 100 = 27,000 \; lbf \, (120,000 \; N)$$

Therefore, the driving force for the TEV must be at least 27,000 lbf (120,000 N) for the normal operation of the TEV.

The tractive effort required, 27,000 lb_f, multiplied by a driving force design factor of 50% (Assumption 3.1.3) yields approximately 40,000 lb_f (178,000 N). Use of the 40,000 lb_f (178,000 N) approximation for the driving force behind the TEV provides a bounding value for the force that a reasonably powered TEV could impart on an emplaced WP in the collision event sequence.

6.3.   FINITE ELEMENT REPRESENTATION

A TEV collision with an emplaced WP is a preclosure event sequence possibility (Reference 2.2.34, Section 4.3.6). The TEV collision event sequence is envisioned as a fully loaded TEV, with doors closed, colliding with an emplaced WP and continuing to drive the WP into yet another emplaced WP. The TEV Collision with an Emplaced WP event sequence is not described in the current *Basis of Design for the TAD Canister-Based Repository Design Concept* (Reference 2.2.10), therefore, the event sequence description provided in *Provisional Event Sequence Definitions for Waste Packages* (Reference 2.2.34) is suitable for its intended use in this calculation. A finite element analysis is performed by using the commercially available LS-DYNA finite element code.

To achieve the largest structural response from this event sequence the 5-DHLW/DOE SNF Short Co-disposal WP, is pushed into the WP with the smallest outer diameter of the expected WP types, the 2-MCO/2-DHLW WP (Assumptions 3.1.1 and 3.2.12). Furthermore, the 2-MCO/2-DHLW WP has boundary conditions applied to it that have it statically positioned at a structurally challenging angle to the 5-DHLW/DOE SNF Co-disposal WP. The angle that the 2-MCO/2-DHLW WP is tilted off of the emplacement drift axis is 30° (Assumption 3.2.13, see section 6.4). Because of the boundary condition applied to the 2-MCO/2-DHLW WP only the top 0.85 meter of the WP is required to be modeled.

The edge of the 2-MCO/2-DHLW WP that will contact the bottom of the 5-DHLW/DOE SNF Short Co-disposal WP during a TEV collision event sequence is placed at two different locations for the simulations that were run. The first position of the 2-MCO/2-DHLW WP contacting edge is in the center of the 5-DHLW/DOE SNF Short Co-disposal WP's OCB bottom lid. The second contacting position simulated has the 2-MCO/2-DHLW WP off center, at the height where a 2-MCO/2-DHLW WP resting on its own pallet would come into contact with an emplaced 5-DHLW/DOE SNF Short Co-disposal WP that was pushed into it, and aligned adjacent to internal basket components that could possibly provide structural resistance. During a TEV collision simulation, if the OCB bottom lid of the 5-DHLW/DOE SNF Short Co-disposal WP were to deform enough to begin loading the inner vessel's bottom lid then a shearing stress possibility could develop

with the placement of the 2-MCO/2-DHLW WP's contacting edge aligned adjacent to the internal basket components.

The TEV is conceptualized in the FER as a simple metal plate approximation for the front doors of the TEV. For this event sequence the TEV doors are in the closed position. The mass assigned to the TEV front doors modeled in the FER is equal to the mass of a fully loaded TEV, at the envelope maximum of 300 *tons* (272,000 *kg*) (Reference 2.2.9, Section 7.8). Plastic material behavior is used for the TEV door conceptualization to maintain more realistic behavior as compared to a simply elastic or rigid material type, and a strong carbon steel material property set for A 516 CS is used to insure a conservative bounding of the TEV door behavior during a collision (Assumption 3.2.14). Because the TEV is on rails, the TEV doors used in the FER have their movement defined so that they can only move in the direction of the emplacement drift axis (z-axis). The TEV has an initial velocity condition of 2.0 *mph* (0.894 *m/s*) toward the emplaced WP (Assumption 3.1.2) and upon contact, a constant force is applied, due to the TEV drive motors, of 40,000 lb_f (178,000 *N*) (Assumption 3.1.3, see Section 6.2).

The pallet that the 5-DHLW/DOE SNF Short Co-disposal WP is resting on is assigned a frictionless boundary condition along its bottom surface. This boundary condition is conservative because a more realistic contact boundary condition between the pallet and the invert surface would dampen the energy from the TEV collision and slow the speed at which the 5-DHLW/DOE SNF Co-disposal WP is pushed into the neighboring WP.

The 5-DHLW/DOE SNF Short Co-disposal WP has the DHLW and DOE SNF canisters conceptualized in the FER. The DHLW is conceptualized with the following parameters: mass = 2,500 kg (5512 lb), length = 3.0 m (118 in), outside diameter = 0.61 m (24 in), canister shell material is 304L stainless steel (Reference 2.2.10, Section 11.2.2.7). In addition to these parameters: neck height = 0.21336 m (8.4 in), neck diameter = 0.1684 m (6.63 in) (Reference 2.2.25, Figure C-20). Note that the use of information from Reference 2.2.25, Figure C-20 is suitable since this has been established as a requirement (Reference 2.2.10, Section 11.2.2.2). The following design parameters are used for the DOE spent nuclear fuel (SNF) canisters (nominally 18 in x 10 ft (0.457 m x 3.048 m)) to be loaded into a 5-DHLW/DOE SNF Short Co-disposal WP: mass = 2,271 kg (5005 lb), length = 3.0 m (118 in), outside diameter = 0.4742 m (18.67 in), canister shell material is 316L stainless steel (Reference 2.2.10, Section 11.2.2.8).

Figures 2 and 3 show the Finite Element Representation (FER) of the TEV Collision with an Emplaced 5-DHLW/DOE SNF Short Co-disposal WP. At the upper end of the 5-DHLW/DOE SNF Short Co-disposal WP the TEV is conceptualized as a 300 *ton* (272,000 *kg*) metal plate. At the lower end of the 5-DHLW/DOE SNF Short Co-disposal WP the upper end of a 2-MCO/2-DHLW WP is conceptualized at an angle of 30° to the emplacement drift axis.

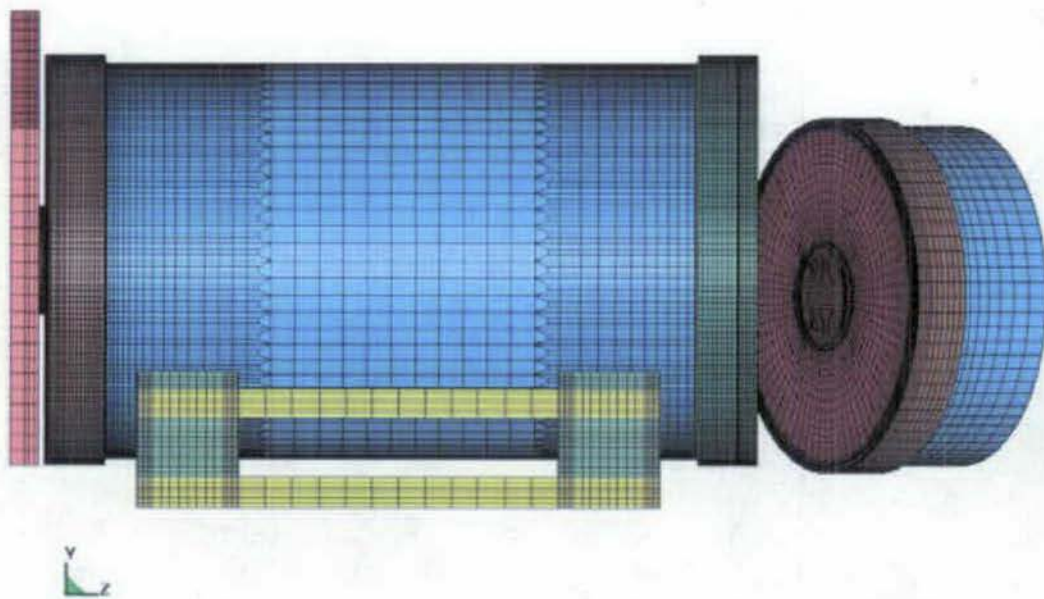**TEV Collision with Emplaced 5 DHLW/DOE**

Figure 2.   FER of a 5-DHLW/DOE SNF Short Co-Disposal WP between a TEV and a
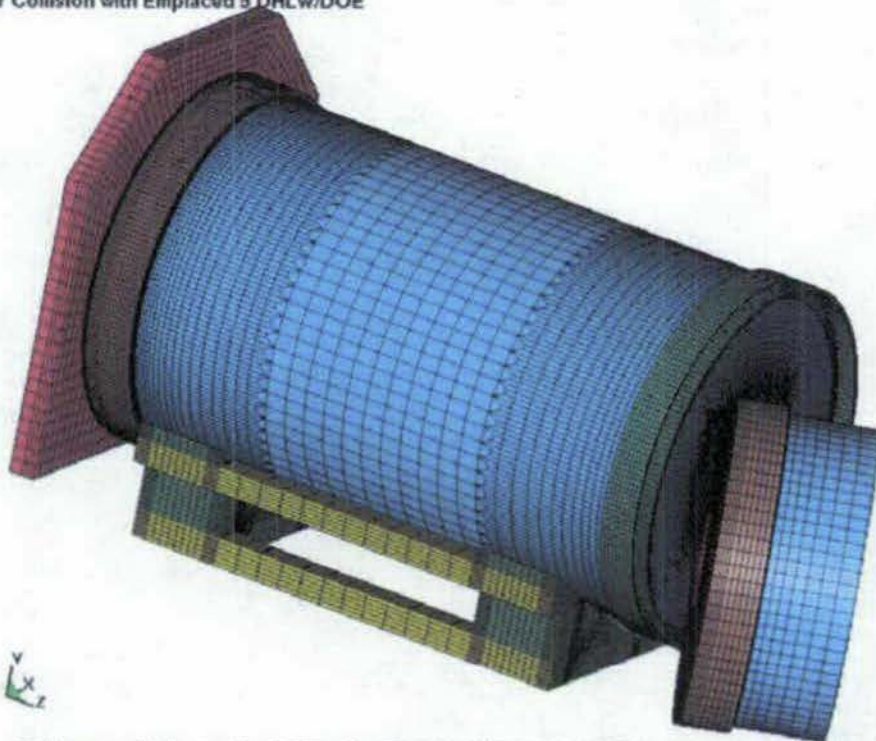2-MCO/2-DHLW WP

TEV Collision with Emplaced 5 DHLW/DOE

Figure 3.   Orthogonal View of a FER of a 5-DHLW/DOE SNF Short Co-Disposal WP between a TEV
and a 2-MCO/2-DHLW WP

August 2007

The 5 DHLW/DOE SNF Short Co-Disposal WP FER is modeled with the inner vessel positioned at the bottom of the OCB cavity. Within the inner vessel there is a FER of loaded DHLW canisters and a DOE SNF canister all positioned toward the bottom of the inner vessel cavity.

LS-DYNA "standard" contact algorithms are used to represent contacts between: OCB and inner vessel, OCB and emplacement pallet and the inner vessel and inner vessel contents. In the absence of more appropriate data, the dynamic friction coefficients for all WP component contacts are assumed to be 0.4 (see Assumption 3.2.8). It is assumed that the functional friction coefficient and the static friction coefficient are equal to the dynamic friction coefficient (see Assumption 3.2.9). To increase solution stability, the contact stiffnesses are doubled and the contact viscous damping is set to 30%. A very small amount of structural damping (*DAMPING_PART_STIFFNESS, Coef = 0.00001) was used to stabilize any high frequency response without any expected affect on the major (low frequency) responses sought after in the OCB.

6.4.   ANGLED POSITION OF THE NEIGHBORING WASTE PACKAGE

The impacted WP is driven into a neighboring WP. For this calculation the neighboring WP is conservatively dimensioned as a 2-MCO/2-DHLW WP (Assumption 3.2.12). The maximum angle at which a 2-MCO/2-DHLW WP can be turned off of the emplacement drift axis, after emplacement, and still be in position to have another emplaced WP driven into its WP sleeve is calculated.

The emplacement drift diameter is 18 *ft* (5.49 *m*) (Reference 2.2.41), so the distance from the furthest drift wall location to the middle of the emplacement drift, or middle of an emplaced package, is the drift radii, 9 *ft* (2.74 *m*).

The 2-MCO/2-DHLW WP length is 207.82 *in* (5.279 *m*) (Reference 2.2.32), minus the lifting feature height of 1.25 *in* (0.0318 *m*) (Reference 2.2.33) gives a WP Sleeve to WP Sleeve length of 206.57 *in* (5.247 *m*).

The angle that a 2-MCO/2-DHLW WP can be turned off of the emplacement drift axis and make contact with the middle of a WP that is driven into it is, θ:

$$\theta = asin(\text{Drift radii/WP length}) = asin(2.74/5.247) = 31.5° \sim 30°$$

7. RESULTS AND CONCLUSIONS

The following results obtained from LS-DYNA are reasonable compared to the inputs and are suitable for the intended use of this calculation.

7.1.   MESH AND TIME STEP VERIFICATION

A study of the FER mesh for the TEV collision into an emplaced WP is performed to verify the objectivity of the mesh, i.e., that the calculation results are not mesh-sensitive. Table 7-1 shows the element wall-averaged (EWA) stress intensity (SI) values for three different FER meshes at the same

relative location on the OCB bottom lid (identified by surface element number) in the region of maximum structural response.

The first (Coarse) mesh in Table 7-1 is developed by following the guidance in *Waste Package Component Design Methodology* (Reference 2.2.28, Section 6.2.3). The Standard mesh is a refined version of the Coarse mesh, where in the region of interest (OCB lower lid) the mesh is refined in the angular coordinate direction. The volumes and stress values for each element are obtained from the post-processing of LS-DYNA simulations. The change in the waste package element volume between the Coarse and Standard mesh is 53%. The change in EWA SI for the elements in the same location is 13%, which indicates that the change in EWA SI is not within acceptability limits described in the Reference 2.2.28, Section 6.2.3. The mesh is again refined to obtain a "Fine" mesh, this time the refinement is performed in the axial (through the thickness of the lid) direction. In the region of interest, the change in volume and EWA stress magnitudes between the Standard and Fine mesh simulations are 40% and 2%, respectively. The level of EWA magnitude change between the Standard mesh and the Fine mesh is low enough to consider either mesh adequate for the purposes of this analysis; no further refinement of the mesh is needed. Since there was little difference between the Standard mesh and the Fine mesh in regards to demand on computing resources, the Fine mesh was used for the simulations performed for this event sequence analysis.

Table 7-1 Mesh Sensitivity Comparison

Coarse Mesh		Standard Mesh		Change from Coarse Mesh
Outer Element # 118950 (OCB bottom lid, at MCO WP contact)	Volume 4.67E-06 m^3 (0.285 in^3)	Outer Element # 155335 (OCB bottom lid, at MCO WP contact)	Volume 2.18E-06 m^3 (0.133 in^3)	53%
	EWA SI 456 MPa (66.1 ksi)		EWA SI 514 MPa (74.5 ksi)	13%
Standard Mesh		Fine Mesh		Change from Standard Mesh
Outer Element # 155335 (OCB bottom lid, at MCO WP contact)	Volume 2.18E-06 m^3 (0.133 in^3)	Outer Element # 188779 (OCB bottom lid, at MCO WP contact)	Volume 1.31E-06 m^3 (0.0799 in^3)	40%
	EWA SI 514 MPa (74.5 ksi)		EWA SI 525 MPa (76.1 ksi)	2%

SI: Stress intensity

7.2. EVALUATION

Table 7-2 contains the maximum calculated EWA SI values in the OCB of the TEV impacted waste package, as well as a comparison of the EWA SI against the true tensile strength of the OCB material (See Section 6.1.2). A comparison between the maximum calculated EWA SI and 0.7 times the true tensile strength of Alloy 22 $(0.7 \, \sigma_u)$ is provided in Table 7-2 to determine if the first condition of acceptance for the EWA SI is met in the tiered acceptance criterion described in Reference 2.2.28, Section 6.2.4. The results indicate that the ratio (EWA SI / $0.7 \, \sigma_u$) is less than 1.0, i.e., the maximum EWA SI at any point in the outer shell and lids does not exceed 0.7 times the true tensile strength of Alloy 22.

Table 7-2 Maximum EWA Stress Intensities

Case Summary	Max EWA SI Outer Element #	EWA SI (*MPa* (*ksi*))	$0.7 \, \sigma_u$	EWA SI / $0.7 \, \sigma_u$
TEV impact 5-DHLW/DOE SNF Short WP, **Center lid Fine Mesh**	e188779	525 (76.1)	0.7 * 971 *MPa* = 680 *MPa* (0.7 * 141 *ksi* = 98.7 *ksi*)	0.77
TEV impact 5-DHLW/DOE SNF Short WP, **Offset on lid Fine Mesh**	e188416	482 (69.9)		0.71

The EWA SI time history plots for each of the maximum EWA SI values reported in Table 7-2 are presented in Figures 4 through 7 in Attachment I. A point of interest in each of the center location simulations (Figures 4 through 6) is the brief EWA SI reduction that occurs between 160*ms* and 180*ms*. Further investigation into this brief EWA SI reduction shows that this is when the inner vessel is first contacted by the indented OCB bottom lid. The inner vessel then recoils a very short distance to the OCB upper lid which makes contact and pushes the inner vessel back down on the indented OCB bottom lid.

7.3. SUMMARY AND CONCLUSION

The output values are reasonable for the given inputs in this calculation. Where uncertainties are not specified, they are taken into account by consistently using the most conservative approach; the calculations, therefore, yield a bounding set of results. The results are suitable for assessment of the stresses in the waste packages. The results presented in Table 7-2 indicate that the maximum EWA SI at any point in the OCB does not exceed 0.7 times the true tensile strength of Alloy 22. The element wall averaged stress response of an emplaced 5-DHLW/DOE SNF Short Co-disposal WP due to a TEV running into it has satisfied the first condition of acceptance of the failure criterion described in Reference 2.2.28, Section 6.2.4 so no further analyses are required. Therefore, the resulting effects of the maximum stresses in the waste package OCB due to a TEV collision event sequence is within acceptable levels and does not cause failure.

ATTACHMENT I.
Figures Obtained From LS-DYNA

Figure 4.   EWA Stress Intensity, Coarse Mesh, OCB Lower Lid, TEV Overdriven Into a 5-DHLW WP
that is Pushed Into a MCO WP Positioned to Contact a Center Location on the Lower Lid

Figure 5.   EWA Stress Intensity, Standard Mesh, OCB Lower Lid, TEV Overdriven Into a 5-DHLW WP
that is Pushed Into a MCO WP Positioned to Contact a Center Location on the Lower Lid

TEV Collision into an Emplaced 5DHLW/DOE SNF Co-Disposal WP, 2MCO/2DHLW WP Positioned Opposite Side Center, Stress Intensity in OCB

EWA SI at e188779, OCB, Bottom Lid

Figure 6.   EWA Stress Intensity, Fine Mesh, OCB Lower Lid, TEV Overdriven Into a 5-DHLW WP that is Pushed Into a MCO WP Positioned to Contact a Center Location on the Lower Lid

TEV Collision into an Emplaced 5DHLW/DOE SNF Co-Disposal WP, 2MCO/2DHLW WP Positioned Opposite Side Off-Center, Stress Intensity in OCB
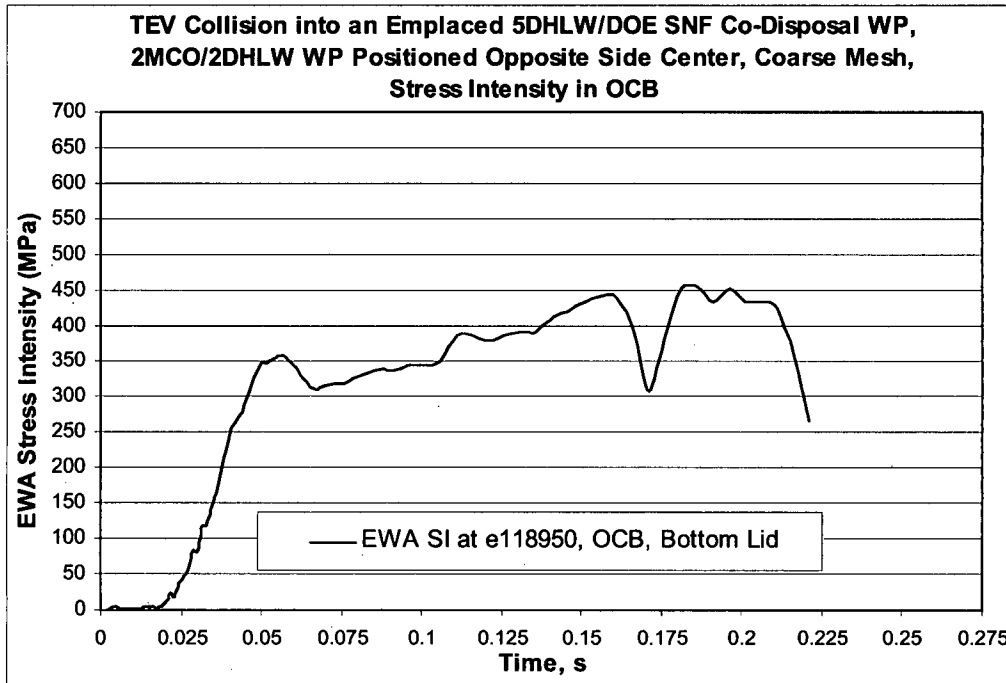
EWA SI at e188416, OCB, Bottom Lid

Figure 7.   EWA Stress Intensity, Fine Mesh, OCB Lower Lid, TEV Overdriven Into a 5-DHLW WP that is Pushed Into a MCO WP Positioned to Contact an Off-Center Location on the Lower Lid
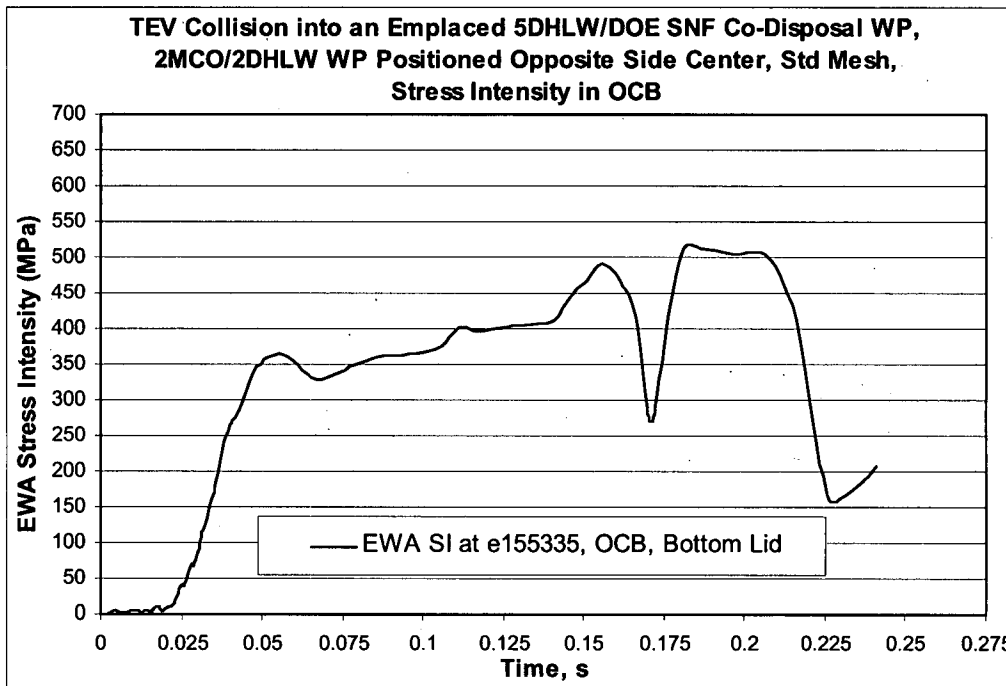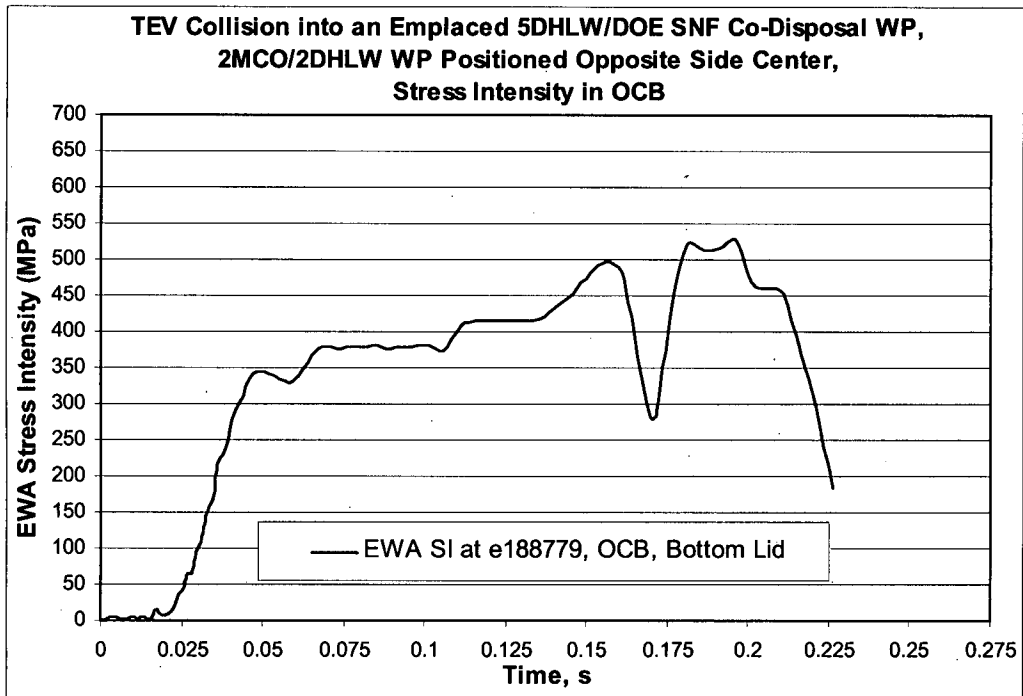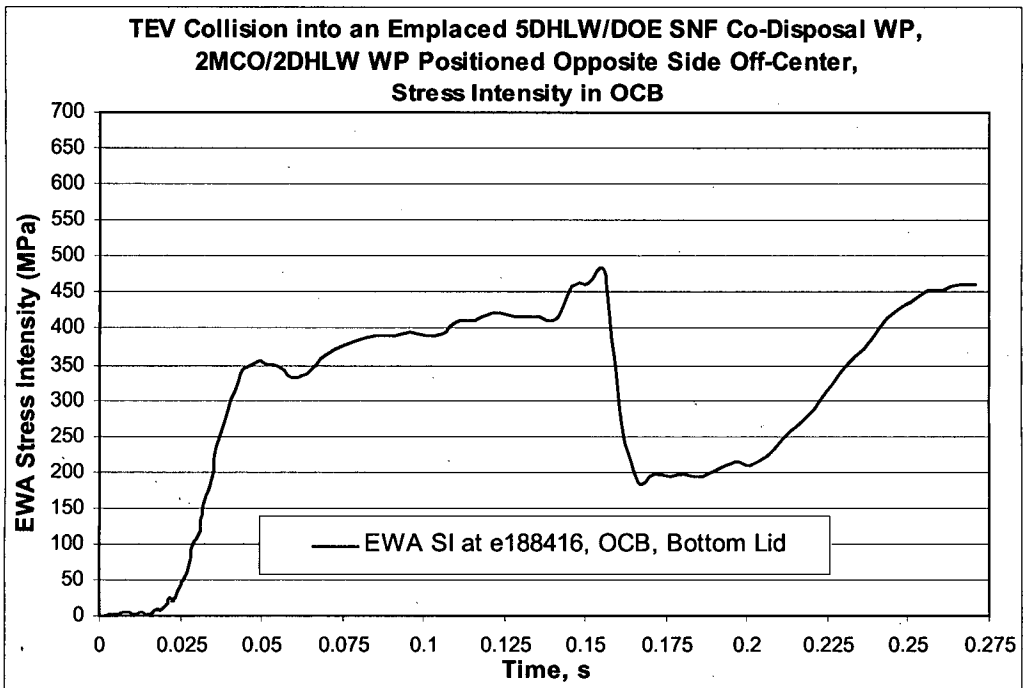
ATTACHMENT II.
Directory Listing (Data CD) of Electronic Files

Table II-1 Attachment II: File Directories, Names, Dates, Times, and Sizes

Directory of D:\

08/23/2007	05:06 PM	<DIR>		CD_Submittal
		0 File(s)	0 bytes	

Directory of D:\CD_Submittal

08/20/2007	09:50 AM	<DIR>		Center_Coarse
08/20/2007	09:51 AM	<DIR>		Center_Fine
08/20/2007	09:50 AM	<DIR>		Center_Standard
08/20/2007	09:52 AM	<DIR>		Off-center_Fine
08/23/2007	05:06 PM		116,736	TEV-into-5DHLW_Plots.xls
		1 File(s)	116,736 bytes	

Directory of D:\CD_Submittal\Center_Coarse

08/20/2007	09:44 AM		81,625,294	d3hsp
08/20/2007	09:44 AM		102,516	glstat
08/20/2007	09:44 AM		41,074	mes0000
08/20/2007	09:44 AM		17,911	mes0001
08/20/2007	09:50 AM	<DIR>		results_center_Coarse
08/16/2007	06:32 PM		28,634,868	TEV_IMPACT_ux_dual13_coars_ctr.inc
08/16/2007	06:32 PM		13,532	TEV_IMPACT_ux_dual13_coars_ctr.k
08/16/2007	06:32 PM		99,068	TEV_IMPACT_ux_dual13_coars_ctr.tg
		7 File(s)	110,534,263 bytes	

Directory of D:\CD_Submittal\Center_Coarse\results_center_Coarse

08/20/2007	08:39 AM		34,902	TEV_coars_OCBbotlid_e118950MSSavg.jpg
08/20/2007	08:39 AM		3,353	TEV_coars_OCBbotlid_e118950MSSavg.txt
08/19/2007	06:26 PM		174	TEV_e118950_Volume.txt
		3 File(s)	38,429 bytes	

Directory of D:\CD_Submittal\Center_Fine

08/13/2007	09:59 AM		117,852,829	d3hsp
08/16/2007	06:37 PM		41,294	mes0000
08/16/2007	06:37 PM		17,946	mes0001
08/23/2007	04:36 PM	<DIR>		results_center_Fine
08/16/2007	06:37 PM		39,330	test.stdout
08/08/2007	11:30 AM		40,557,155	TEV_IMPACT_ux_dual13_ctr.inc
08/08/2007	11:30 AM		13,430	TEV_IMPACT_ux_dual13_ctr.k
08/08/2007	11:30 AM		99,055	TEV_IMPACT_ux_dual13_ctr.tg
		7 File(s)	158,621,039 bytes	

Directory of D:\CD_Submittal\Center_Fine\results_center_Fine

08/14/2007	05:25 PM		954	156ms_results_188779High.txt
08/14/2007	05:25 PM		954	181ms_results_191776High.txt
08/14/2007	05:25 PM		954	186ms_results_188779High.txt
08/14/2007	05:25 PM		954	196ms_results_188779HighHigh.txt
08/14/2007	05:24 PM		3,394	TEV_ctr_OCB-Botlid_188617MSSavg.txt
08/14/2007	05:24 PM		3,394	TEV_ctr_OCB-Botlid_188752MSSavg.txt
08/14/2007	05:24 PM		3,394	TEV_ctr_OCB-Botlid_188752MSSavg2.txt

August 2007

```
08/14/2007  05:24 PM          35,346 TEV_ctr_OCB-Botlid_188779MSSavg.jpg
08/14/2007  05:24 PM           3,394 TEV_ctr_OCB-Botlid_188779MSSavg2.txt
08/14/2007  05:24 PM           3,394 TEV_ctr_OCB-Botlid_188806MSSavg2.txt
08/14/2007  05:24 PM           3,394 TEV_ctr_OCB-Botlid_188833MSSavg.txt
08/14/2007  05:24 PM           3,394 TEV_ctr_OCB-Botlid_191776MSSavg2.txt
08/14/2007  05:24 PM           3,394 TEV_ctr_OCB-Botlid_191803MSSavg2.txt
08/14/2007  05:24 PM           3,394 TEV_ctr_OCB-Botlid_191830MSSavg2.txt
08/14/2007  05:24 PM           3,394 TEV_ctr_OCB-Botlid_191857MSSavg2.txt
08/14/2007  05:24 PM           3,394 TEV_ctr_OCB-Botlid_191937MSSavg2.txt
08/23/2007  04:36 PM           3,398 TEV_ctr_OCB-Botlid_MCO-push_188779EffPlaStrnAvg.txt
              17 File(s)      79,894 bytes

Directory of D:\CD_Submittal\Center_Standard

08/20/2007  09:48 AM     109,241,657 d3hsp
08/20/2007  09:47 AM         111,656 glstat
08/20/2007  09:47 AM          42,714 mes0000
08/20/2007  09:47 AM          18,218 mes0001
08/20/2007  09:50 AM    <DIR>        results_center_Standard
08/16/2007  06:32 PM      33,646,158 TEV_IMPACT_ux_dual13_std_ctr.inc
08/16/2007  06:32 PM          13,530 TEV_IMPACT_ux_dual13_std_ctr.k
08/16/2007  06:32 PM          99,055 TEV_IMPACT_ux_dual13_std_ctr.tg
               7 File(s)   143,172,988 bytes

Directory of D:\CD_Submittal\Center_Standard\results_center_Standard

08/20/2007  08:39 AM          36,244 TEV_std_ctrocb_botlid_155335MSSavg.jpg
08/20/2007  08:39 AM           3,517 TEV_std_ctrocb_botlid_155335MSSavg.txt
08/19/2007  06:26 PM           2,143 TEV_std_e155335_Volume.txt
               3 File(s)      41,904 bytes

Directory of D:\CD_Submittal\Off-center_Fine

08/13/2007  10:12 AM     115,263,948 d3hsp
08/16/2007  06:34 PM         124,452 glstat
08/16/2007  06:34 PM          44,358 mes0000
08/16/2007  06:34 PM          18,253 mes0001
08/20/2007  09:15 AM    <DIR>        results_offcenter_Fine
08/16/2007  06:33 PM          42,618 test.stdout
08/08/2007  11:30 AM      40,532,372 TEV_IMPACT_ux_dual13.inc
08/08/2007  11:30 AM          13,426 TEV_IMPACT_ux_dual13.k
08/08/2007  11:30 AM          98,986 TEV_IMPACT_ux_dual13.tg
               8 File(s)   156,138,413 bytes

Directory of D:\CD_Submittal\Off-center_Fine\results_offcenter_Fine

08/14/2007  04:46 PM           1,563 146ms_results_188497High.txt
08/14/2007  04:46 PM           1,567 146ms_results_188497Highb.txt
08/14/2007  04:46 PM           1,567 151ms_results_188497Highb.txt
08/14/2007  04:46 PM           1,567 156ms_results_188416HighbHigh.txt
08/14/2007  04:46 PM           1,235 161ms_results_188740High.txt
08/14/2007  04:46 PM          34,662 TEV-188740MSSavg.jpg
08/14/2007  04:46 PM           3,763 TEV-offset_OCB-botLid_188225MSSavg.txt
08/14/2007  04:46 PM           3,763 TEV-offset_OCB-botLid_188254MSSavg.txt
08/14/2007  04:46 PM           3,763 TEV-offset_OCB-botLid_188362MSSavg.txt
08/14/2007  04:46 PM           3,763 TEV-offset_OCB-botLid_188389MSSavg.txt
08/14/2007  04:46 PM           3,763 TEV-offset_OCB-botLid_188416MSSavg.txt
08/14/2007  04:46 PM           3,763 TEV-offset_OCB-botLid_188443MSSavg.txt
08/14/2007  04:46 PM           3,763 TEV-offset_OCB-botLid_188497MSSavg.txt
08/14/2007  04:46 PM           3,763 TEV-offset_OCB-botLid_188524MSSavg.txt
08/14/2007  04:46 PM           3,763 TEV-offset_OCB-botLid_188551MSSavg.txt
08/14/2007  04:46 PM           3,722 TEV-offset_OCB-botLid_188551MSSavg2.txt
```

```
08/14/2007  04:46 PM        3,722 TEV-offset_OCB-botLid_188578MSSavg.txt
08/14/2007  04:46 PM        3,763 TEV-offset_OCB-botLid_188605MSSavg.txt
08/14/2007  04:46 PM        3,763 TEV-offset_OCB-botLid_188659MSSavg.txt
08/14/2007  04:46 PM        3,763 TEV-offset_OCB-botLid_188713MSSavg.txt
08/14/2007  04:46 PM        3,763 TEV-offset_OCB-botLid_188713MSSavg2.txt
08/14/2007  04:46 PM        3,763 TEV-offset_OCB-botLid_188740MSSavg.txt
08/14/2007  04:46 PM        3,763 TEV-offset_OCB-botLid_188767MSSavg.txt
08/14/2007  04:46 PM        3,763 TEV-offset_OCB-botLid_188794MSSavg.txt
08/14/2007  04:46 PM        3,722 TEV-offset_OCB-botLid_edge_164254MSSavg.txt
08/14/2007  04:46 PM        3,721 TEV-offset_OCB-Toplid_edge_40438MSSav.txt
08/14/2007  04:46 PM        3,721 TEV-offset_OCBlid_edgespan_33243MSSav.txt
08/14/2007  04:46 PM        3,721 TEV-offset_OCBlid_innerspan_33229MSSav.txt
08/14/2007  04:46 PM        3,721 TEV-offset_OCBlid_midspan_33237MSSavg.txt
08/14/2007  04:46 PM        3,721 TEV-offset_OCBshellTop_93779MSSavg.txt
                30 File(s)     132,140 bytes
```

NOTE: The file order, sizes (bytes) and times may vary with operating system.

This is a placeholder page for records that cannot be scanned.

2. Record Date	3. Accession Number
08/30/2007	ATT TO: ENG.20070904.0033

4. Author Name(s)	5. Authorization Organization
Bryan Dunlap	RPM/Thermal/Structural Analysis

6. Title/Description

TEV Collision with an Emplaced 5-DHLW/DOE SNF Short Co-disposal Waste Package

7. Document Number(s)	8. Version Designator
000-00C-MGR0-04100-000	00A

9. Document Type	10. Medium
Media	2 CD's

11. Access Control Code

N/A

12. Traceability Designator

000-00C-MGR0-04100-000-00A

13. Comments

CD'S: 1 Original
     1 Copy

Validation of complete file transferred. All files copied. Software used: LS-DYNA V.970.3858 D MPP; TrueGrid V2.2; LS-PREPOST V1.0; Microsoft Office Excel 2003

14. RPC Electronic Media Verification

MOL.20070904.0010

XREF

SEP 0 6 2007   TChurch /BSC-BS

MD5 Validation

THIS IS AN ELECTRONIC
ATTACHMENT

```
Volume in drive D is 070827_1158
Volume Serial Number is C4F9-8313

Directory of D:\

08/23/2007  05:06p      <DIR>           CD_Submittal
              0 File(s)              0 bytes

Directory of D:\CD_Submittal

08/23/2007  05:06p      <DIR>           .
08/28/2007  09:10a      <DIR>           ..
08/20/2007  09:50a      <DIR>           Center_Coarse
08/20/2007  09:51a      <DIR>           Center_Fine
08/20/2007  09:50a      <DIR>           Center_Standard
08/20/2007  09:52a      <DIR>           Off-center_Fine
08/23/2007  05:06p          116,736 TEV-into-5DHLW_Plots.xls
              1 File(s)        116,736 bytes

Directory of D:\CD_Submittal\Center_Coarse

08/20/2007  09:50a      <DIR>           .
08/23/2007  05:06p      <DIR>           ..
08/20/2007  09:44a       81,625,294 d3hsp
08/20/2007  09:44a          102,516 glstat
08/20/2007  09:44a           41,074 mes0000
08/20/2007  09:44a           17,911 mes0001
08/20/2007  09:50a      <DIR>           results_center_Coarse
08/16/2007  06:32p       28,634,868 TEV_IMPACT_ux_dual13_coars_ctr.inc
08/16/2007  06:32p           13,532 TEV_IMPACT_ux_dual13_coars_ctr.k
08/16/2007  06:32p           99,068 TEV_IMPACT_ux_dual13_coars_ctr.tg
              7 File(s)    110,534,263 bytes

Directory of D:\CD_Submittal\Center_Coarse\results_center_Coarse

08/20/2007  09:50a      <DIR>           .
08/20/2007  09:50a      <DIR>           ..
08/20/2007  08:39a           34,902 TEV_coars_OCBbotlid_e118950MSSavg.jpg
08/20/2007  08:39a            3,353 TEV_coars_OCBbotlid_e118950MSSavg.txt
08/19/2007  06:26p              174 TEV_e118950_Volume.txt
              3 File(s)         38,429 bytes

Directory of D:\CD_Submittal\Center_Fine

08/20/2007  09:51a      <DIR>           .
08/23/2007  05:06p      <DIR>           ..
08/13/2007  09:59a      117,852,829 d3hsp
08/16/2007  06:37p           41,294 mes0000
08/16/2007  06:37p           17,946 mes0001
08/23/2007  04:36p      <DIR>           results_center_Fine
08/16/2007  06:37p           39,330 test.stdout
08/08/2007  11:30a       40,557,155 TEV_IMPACT_ux_dual13_ctr.inc
08/08/2007  11:30a           13,430 TEV_IMPACT_ux_dual13_ctr.k
08/08/2007  11:30a           99,055 TEV_IMPACT_ux_dual13_ctr.tg
              7 File(s)    158,621,039 bytes

Directory of D:\CD_Submittal\Center_Fine\results_center_Fine

08/23/2007  04:36p      <DIR>           .
08/20/2007  09:51a      <DIR>           ..
08/14/2007  05:25p              954 156ms_results_188779High.txt
08/14/2007  05:25p              954 181ms_results_191776High.txt
08/14/2007  05:25p              954 186ms_results_188779High.txt
```

```
                                         dir.txt
08/14/2007   05:25p                    954 196ms_results_188779HighHigh.txt
08/14/2007   05:24p                  3,394 TEV_ctr_OCB-Botlid_188617MSSavg.txt
08/14/2007   05:24p                  3,394 TEV_ctr_OCB-Botlid_188752MSSavg.txt
08/14/2007   05:24p                  3,394 TEV_ctr_OCB-Botlid_188752MSSavg2.txt
08/14/2007   05:24p                 35,346 TEV_ctr_OCB-Botlid_188779MSSavg.jpg
08/14/2007   05:24p                  3,394 TEV_ctr_OCB-Botlid_188779MSSavg2.txt
08/14/2007   05:24p                  3,394 TEV_ctr_OCB-Botlid_188806MSSavg2.txt
08/14/2007   05:24p                  3,394 TEV_ctr_OCB-Botlid_188833MSSavg.txt
08/14/2007   05:24p                  3,394 TEV_ctr_OCB-Botlid_191776MSSavg2.txt
08/14/2007   05:24p                  3,394 TEV_ctr_OCB-Botlid_191803MSSavg2.txt
08/14/2007   05:24p                  3,394 TEV_ctr_OCB-Botlid_191830MSSavg2.txt
08/14/2007   05:24p                  3,394 TEV_ctr_OCB-Botlid_191857MSSavg2.txt
08/14/2007   05:24p                  3,394 TEV_ctr_OCB-Botlid_191937MSSavg2.txt
08/23/2007   04:36p                  3,398
TEV_ctr_OCB-Botlid_MCO-push_188779EffPlaStrnAvg.txt
              17 File(s)         79,894 bytes

    Directory of D:\CD_Submittal\Center_Standard

08/20/2007   09:50a     <DIR>            .
08/23/2007   05:06p     <DIR>            ..
08/20/2007   09:48a        109,241,657 d3hsp
08/20/2007   09:47a            111,656 glstat
08/20/2007   09:47a             42,714 mes0000
08/20/2007   09:47a             18,218 mes0001
08/20/2007   09:50a     <DIR>            results_center_Standard
08/16/2007   06:32p         33,646,158 TEV_IMPACT_ux_dual13_std_ctr.inc
08/16/2007   06:32p             13,530 TEV_IMPACT_ux_dual13_std_ctr.k
08/16/2007   06:32p             99,055 TEV_IMPACT_ux_dual13_std_ctr.tg
               7 File(s)    143,172,988 bytes

    Directory of D:\CD_Submittal\Center_Standard\results_center_Standard

08/20/2007   09:50a     <DIR>            .
08/20/2007   09:50a     <DIR>            ..
08/20/2007   08:39a             36,244 TEV_std_ctrocb_botlid_155335MSSavg.jpg
08/20/2007   08:39a              3,517 TEV_std_ctrocb_botlid_155335MSSavg.txt
08/19/2007   06:26p              2,143 TEV_std_e155335_Volume.txt
               3 File(s)         41,904 bytes

    Directory of D:\CD_Submittal\Off-center_Fine

08/20/2007   09:52a     <DIR>            .
08/23/2007   05:06p     <DIR>            ..
08/13/2007   10:12a        115,263,948 d3hsp
08/16/2007   06:34p            124,452 glstat
08/16/2007   06:34p             44,358 mes0000
08/16/2007   06:34p             18,253 mes0001
08/20/2007   09:15a     <DIR>            results_offcenter_Fine
08/16/2007   06:33p             42,618 test.stdout
08/08/2007   11:30a         40,532,372 TEV_IMPACT_ux_dual13.inc
08/08/2007   11:30a             13,426 TEV_IMPACT_ux_dual13.k
08/08/2007   11:30a             98,986 TEV_IMPACT_ux_dual13.tg
               8 File(s)    156,138,413 bytes

    Directory of D:\CD_Submittal\Off-center_Fine\results_offcenter_Fine

08/20/2007   09:15a     <DIR>            .
08/20/2007   09:52a     <DIR>            ..
08/14/2007   04:46p              1,563 146ms_results_188497High.txt
08/14/2007   04:46p              1,567 146ms_results_188497Highb.txt
08/14/2007   04:46p              1,567 151ms_results_188497Highb.txt
08/14/2007   04:46p              1,567 156ms_results_188416HighbHigh.txt
```

dir.txt

08/14/2007	04:46p	1,235	161ms_results_188740High.txt
08/14/2007	04:46p	34,662	TEV-188740MSSavg.jpg
08/14/2007	04:46p	3,763	TEV-offset_OCB-botLid_188225MSSavg.txt
08/14/2007	04:46p	3,763	TEV-offset_OCB-botLid_188254MSSavg.txt
08/14/2007	04:46p	3,763	TEV-offset_OCB-botLid_188362MSSavg.txt
08/14/2007	04:46p	3,763	TEV-offset_OCB-botLid_188389MSSavg.txt
08/14/2007	04:46p	3,763	TEV-offset_OCB-botLid_188416MSSavg.txt
08/14/2007	04:46p	3,763	TEV-offset_OCB-botLid_188443MSSavg.txt
08/14/2007	04:46p	3,763	TEV-offset_OCB-botLid_188497MSSavg.txt
08/14/2007	04:46p	3,763	TEV-offset_OCB-botLid_188524MSSavg.txt
08/14/2007	04:46p	3,763	TEV-offset_OCB-botLid_188551MSSavg.txt
08/14/2007	04:46p	3,722	TEV-offset_OCB-botLid_188551MSSavg2.txt
08/14/2007	04:46p	3,722	TEV-offset_OCB-botLid_188578MSSavg.txt
08/14/2007	04:46p	3,763	TEV-offset_OCB-botLid_188605MSSavg.txt
08/14/2007	04:46p	3,763	TEV-offset_OCB-botLid_188659MSSavg.txt
08/14/2007	04:46p	3,763	TEV-offset_OCB-botLid_188713MSSavg.txt
08/14/2007	04:46p	3,763	TEV-offset_OCB-botLid_188713MSSavg2.txt
08/14/2007	04:46p	3,763	TEV-offset_OCB-botLid_188740MSSavg.txt
08/14/2007	04:46p	3,763	TEV-offset_OCB-botLid_188767MSSavg.txt
08/14/2007	04:46p	3,763	TEV-offset_OCB-botLid_188794MSSavg.txt
08/14/2007	04:46p	3,722	TEV-offset_OCB-botLid_edge_164254MSSavg.txt
08/14/2007	04:46p	3,721	TEV-offset_OCB-Toplid_edge_40438MSSav.txt
08/14/2007	04:46p	3,721	TEV-offset_OCBlid_edgespan_33243MSSav.txt
08/14/2007	04:46p	3,721	TEV-offset_OCBlid_innerspan_33229MSSav.txt
08/14/2007	04:46p	3,721	TEV-offset_OCBlid_midspan_33237MSSavg.txt
08/14/2007	04:46p	3,721	TEV-offset_OCBshellTop_93779MSSavg.txt

```
              30 File(s)        132,140 bytes

   Total Files Listed:
           83 File(s)    568,875,806 bytes
           27 Dir(s)               0 bytes free
```